arXiv:nucl-th/0411043v1 11 Nov 2004

Skewed recoil polarization in $(e, e'p)$ reactions from polarized nuclei

J.E. Amaro[1], M.B. Barbaro[2], J.A. Caballero[3]

[1] *Departamento de Física Moderna, Universidad de Granada, Granada 18071, Spain*

[2] *Dipartimento di Fisica Teorica, Università di Torino and INFN, Sezione di Torino Via P. Giuria 1, 10125 Torino, ITALY*

[3] *Departamento de Física Atómica, Molecular y Nuclear Universidad de Sevilla, Apdo. 1065, E-41080 Sevilla, SPAIN*

Abstract

The general formalism describing $\vec{A}(\vec{e}, e'\vec{p})B$ reactions, involving polarization of the electron beam, target and ejected proton, is presented within the framework of the relativistic plane wave impulse approximation for medium and heavy nuclei. It is shown that the simultaneous measurement of the target and ejected proton polarization can provide new information which is not contained in the separate analysis of the $\vec{A}(\vec{e}, e'p)B$ and $A(\vec{e}, e'\vec{p})B$ reactions. The polarization transfer mechanism in which the electron interacts with the initial nucleon carrying the target polarization, making the proton exit with a fractional polarization in a different direction, is referred to here as "skewed polarization". The new observables characterizing the process are identified, and written in terms of polarized response functions and asymmetries which are of tensor nature. The corresponding half-off-shell single-nucleon responses are analyzed using different prescriptions for the electromagnetic vertex and for different kinematics. Numerical predictions are presented for selected perpendicular and parallel kinematics in the case of ^{39}K as polarized target.

PACS: 25.30.Fj, 24.10.Jv, 24.70.+s

Keywords: Nuclear reactions; Coincidence electron scattering; Polarization transfer; Response functions; Polarized momentum distribution.

1 Introduction

It is well known that polarization degrees of freedom in electron scattering reactions lead to new observables which provide additional information on the nuclear structure as well as on the reaction mechanism [1, 2, 3, 4]. In general, the control of leptonic and hadronic polarizations allows new combinations of electromagnetic multipole matrix elements that show different sensitivities to the diverse ingredients entering in the description of the reaction mechanism.

In inclusive $(\vec{e}, e')$ processes, the polarization of the incident lepton yields information not only on the nucleonic structure (in particular the strange and axial nucleon's form factors, see e.g. refs. [5, 6]), but also on some specific nuclear correlations which are not probed by unpolarized electrons [7, 8, 9, 10].

In recent years a great effort, both from experimental and theoretical points of view, has been devoted to the analysis of exclusive $(e, e'p)$ with leptonic and/or hadronic polarization measurements for medium nuclei. This has been for instance the case of $(e, e'\vec{p})$ processes and the measurement of induced polarization [11, 12] as it crucially depends on final state interactions (FSI) (the induced polarization is zero in the plane wave limit) [13, 14, 15, 16, 17, 18, 19]. Double polarized $(\vec{e}, e'\vec{p})$ experiments have been also carried out to measure polarization transfer asymmetries for medium [20, 21] and light nuclei [22, 23], as they may provide information on the possible modifications of the nucleon form factors in the nuclear interior [15, 24]. Finally, the case of electron scattering on polarized targets, i.e., $\vec{A}(e, e'p)$ and $\vec{A}(\vec{e}, e'p)$ processes, has been analyzed as well from the theoretical point of view for medium nuclei in a number of papers [25, 26, 27, 28, 29, 30] and, in particular, important connections between FSI and the nuclear polarization direction have been found [31, 32].

However studies of spin observables in $\vec{A}(\vec{e}, e'\vec{p})$ when the beam, target and final nucleon are simultaneously polarized exist only scarcely. Apart from the general approach of ref. [2], research on these reactions has only been performed for light nuclei. In particular it is worth mentioning the systematic research on general sets of spin observables for deuterium performed in the last decade by Arenhövel *et al.* [33, 34, 35, 36, 37, 38]. In the present paper we try to fill this gap and begin an exploration of the new spin observables that arise in these exclusive reactions from medium nuclei. Although no experiments of this kind are presently under planning, theoretical studies of such reactions are needed to gauge the magnitude and properties of the new observables, and to determine if new relevant physical information can be extracted from them. Accordingly, in this work we focus on a new polarization mechanism of the recoil proton, which is absent in the reactions previously studied. In fact, for unpolarized nuclei, there are two such mechanisms: (i) For unpolarized electrons *induced polarization* is produced on the recoil protons by effect of the FSI with the residual nucleus.

In DWIA models [39] this effect is partially due to the imaginary part of the central optical potential —which produces different absorptions for protons exiting from regions of the nucleus with different local spin directions— and partially due to the spin-orbit potential, which produces a spin-dependent interaction. (ii) Polarized electrons can transfer part of their spin to the nucleon. Thus *polarization transfer* arises already within the plane wave limit and FSI are proved not to affect appreciably these observables for low missing momentum [24, 40]. In the case of unpolarized electrons on polarized nuclei another mechanism takes place, namely the polarization transfer from the target to the final proton. In some cases of interest, a semi-classical interpretation of the reaction mechanism producing such polarization transfer can be drawn. In fact, in the case of knock-out from the outer shell, the initial proton is carrying part of the nuclear polarization, so an expected value of the initial spin can be defined for the proton [32, 39]. In general, the final direction of the recoil polarization does not coincide with the initial one, so the interaction is producing a change of the proton spin. The effect of the electromagnetic interaction is then to pull the proton with a twist of its spin, so the final proton results partially polarized in a direction different from the initial one. We call this effect "skewed polarization", to distinguish it from the term "polarization transfer" normally used for polarized electrons. The corresponding hadronic observables, namely response functions and recoil polarization asymmetries, can be represented by tensor quantities. One of the goals of this paper is to present predictions for the polarization asymmetries that can be measured in these reactions for different polarization directions and to identify the situations in which large recoil polarizations are expected in a typical experiment.

It is well known that FSI constitute an essential ingredient in order to analyze experimental data (cross sections and/or response functions) in detail. Some specific polarized and unpolarized responses are strictly zero in the plane wave limit; hence these observables may help to constrain theoretical uncertainties in the treatment of FSI. However, although being aware of the importance of FSI or other effects due to ingredients beyond the impulse approximation such as meson exchange currents (MEC), in this work we restrict our analysis to the plane wave impulse approximation (PWIA) in a first approach to the problem. As already noted in refs. [26, 41, 42, 43], this particularly simple description allows one to simplify and clarify the essential physical issues underlying the problem. Moreover, some observables given as ratios of cross sections and/or response functions are shown to be rather insensitive to FSI and other distortion effects, and thus PWIA calculations may be adequate.

In spite of its simplicity, PWIA has proved its capability for the interpretation of experimental data. One of the basic advantages of PWIA is that the cross sections, and consequently the response functions, factorize into a single-nucleon cross section, dealing directly with the interaction between the incident electrons and the bound nucleons inside

the nucleus, and a spectral function which gives the probability to find a nucleon in the nucleus with given energy and momentum. Both terms may in turn be functions of the spin variables involved in the reaction. The importance of factorization lies on the fact that experimental data are still usually interpreted making use of an *effective* spectral function that is extracted from experiment. A systematic study of the validity of factorization within the general framework of the relativistic distorted wave impulse approximation (RDWIA) has been presented recently in [44]. It has been shown that exact factorization also emerges with FSI under very restrictive assumptions on the relativistic dynamics and spin dependence in the problem. For some observables, evaluated as ratios of cross sections, and not too high values of the missing momentum, it has been proved that the *factorized* PWIA results are in accordance with much more sophisticated and *unfactorized* calculations which include FSI. These ideas apply to the skewed polarization asymmetries analyzed in this paper, since these observables arise already in PWIA: hence one expects the effect of FSI to be small on these, at least for low values of the missing momentum.

In this paper we follow closely the formalism developed in [26, 28] for the case of $\vec{A}(\vec{e}, e'p)$, i.e., scattering on polarized targets, and in [43] for outgoing nucleon polarization reactions $A(\vec{e}, e'\vec{p})$. Here we extend the analysis and consider the case of target and outgoing nucleon polarizations measured simultaneously. Obviously, the single nucleon responses entering into the analysis of $\vec{A}(\vec{e}, e'\vec{p})$ reactions contain as particular cases those ones entering into the separate descriptions of $A(\vec{e}, e'\vec{p})$ and $\vec{A}(\vec{e}, e'p)$ processes. Therefore we focus on the "new" response functions, which depend on both the target and ejected nucleon polarizations.

A basic ingredient of PWIA deals with the single-nucleon response functions and how they depend on the off-shell effects for different kinematics. In this paper we perform a study of these effects on the new response functions following the approach originally introduced by de Forest [45]. We make use of the two standard forms for the γNN vertex and consider various prescriptions for restoring current conservation.

As a second step, in order to obtain the nuclear coincidence cross section or hadronic responses one also needs the polarized spectral function, which depends on the target polarization, to be multiplied by the polarized single-nucleon cross section/responses. This is written in terms of a partial momentum distribution, that depends on the particular initial and daugther nuclear states. In this work we present results for the case of a typical medium nucleus that can be polarized, namely the ^{39}K nucleus, which is described in shell model as a proton hole in the $d_{3/2}$ shell of ^{40}Ca.

The general structure of the paper is as follows. In Section 2 we briefly review the basic formalism for $\vec{A}(\vec{e}, e'\vec{p})$ reactions focusing on the PWIA. Here we evaluate the single-nucleon tensor and analyze its dependence on the spin variables. In Section 3 we present the results: first we focus on the single-nucleon responses, where off-shell effects and symmetry

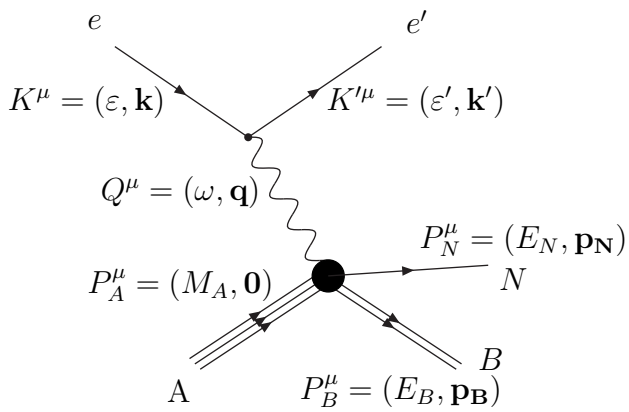

Figure 1: Feynman diagram for the $A(e, e'N)B$ process within the Born approximation.

properties are carefully studied; second we present our predictions for final observables, namely "skewed" polarization asymmetries, for ^{39}K. Finally in Section 4 we summarize our conclusions. The detailed expressions of the single nucleon tensors, responses and momentum distribution are given in the Appendices.

2 Formalism of $\vec{A}(\vec{e}, e'\vec{p})B$ reactions

In this section we summarize the basic formalism involved in the description of coincidence $(e, e'p)$ reactions [2]. The Feynman diagram within the Born approximation (one virtual photon exchange) is depicted in Fig. 1 and defines our conventions on energies and momenta. In what follows we introduce the kinematical variables that completely specify the process and use energy-momentum conservation to inter-relate the various energies and momenta:

$$\mathbf{q} = \mathbf{k} - \mathbf{k}' = \mathbf{p}_N + \mathbf{p}_B \tag{1}$$

$$\omega = \varepsilon - \varepsilon' = E_B + E_N - M_A \,, \tag{2}$$

where the target is assumed to be at rest in the laboratory frame. The missing momentum $\mathbf{p}$ is defined as

$$\mathbf{p} \equiv -\mathbf{p}_B = \mathbf{p}_N - \mathbf{q} \,. \tag{3}$$

The general form for the coincidence cross section in the laboratory system is

$$\frac{d\sigma}{d\Omega_e d\varepsilon' d\Omega_N} = \frac{2\alpha^2}{Q^4} \left(\frac{\varepsilon'}{\varepsilon}\right) K f_{rec}^{-1} \eta_{\mu\nu} W^{\mu\nu} \,, \tag{4}$$

where $K = p_N M_N M_B / M_A$, α is the fine structure constant, f_{rec} is the usual recoil factor [2], $\eta_{\mu\nu}$ is the leptonic tensor that can be evaluated using trace techniques [2], and $W^{\mu\nu}$ is the hadronic tensor containing all of the nuclear structure and dynamics information. The latter is given in terms of the nuclear electromagnetic transition currents in momentum space. Note that the above equation is completely general and may contain all polarization degrees of freedom. The electron beam polarization occurs in the antisymmetric part of the leptonic tensor $\eta_{\mu\nu}$, while the target and recoil nucleon polarizations enter through the hadronic tensor $W^{\mu\nu}$.

Using the general properties of the leptonic tensor, the contraction of the leptonic and hadronic tensors can be decomposed in terms of leptonic kinematical "super-Rosenbluth" factors and response functions. The differential cross section can then be written as

$$\frac{d\sigma}{d\Omega_e d\varepsilon' d\Omega_N} = \Sigma + h\Delta \,, \tag{5}$$

being

$$\begin{aligned} \Sigma &= K\sigma_M f_{rec}^{-1} \left(v_L R^L + v_T R^T + v_{TL} R^{TL} + v_{TT} R^{TT} \right) \\ \Delta &= K\sigma_M f_{rec}^{-1} \left(v_{T'} R^{T'} + v_{TL'} R^{TL'} \right) \,, \end{aligned} \tag{6}$$

where σ_M is the Mott cross section. The kinematic factors v_α contain all of the dependence on the leptonic vertex aside from overall multiplicative factors (see [2] for their explicit expressions in the extreme relativistic limit). The factor $h = \pm 1$ is the incident electron's helicity. The hadronic current enters via the response functions R^α, which thus contain all the information on the target and ejected nucleon spin dependence. The labels L and T refer to projections of the current matrix elements longitudinal and transverse to the virtual photon direction, respectively.

2.1 Plane-Wave Impulse Approximation (PWIA)

The PWIA constitutes the simplest approach to describing the reaction mechanism for coincidence electron scattering reactions. It has been discussed in detail in previous work [1, 3, 4, 26], and thus here we simply summarize the basic expressions needed for the discussion to follow. The basic assumptions in PWIA are the following: i) the electromagnetic current is taken to be a one-body operator (impulse approximation), ii) the ejected nucleon is a plane wave, i.e., the nucleon emerges from the nucleus without interaction with the residual nuclear system, and iii) the nucleon detected in the coincidence reaction is the one to which the virtual photon is attached. Thus, the hadronic final state in PWIA is simply characterized by the product of the state of the residual nucleus $|B\rangle$ and the on-shell knocked-out

nucleon spinor state $|\mathbf{p}_N, S_N\rangle$. Moreover, the momentum of the struck nucleon coincides with the missing momentum defined in Eq. (3). The hadronic tensor can then be written in the general form:

$$W^{\mu\nu} = \sum_{mm'} \mathcal{W}^{\mu\nu}_{mm'}(\mathbf{p}, \mathbf{q}; S_N) M_{mm'}(\mathbf{p}, \mathbf{\Omega}^*) \,, \tag{7}$$

where S_N refers to the ejected nucleon four-spin and $\mathbf{\Omega}^*$ defines the target polarization direction. The tensor in (7) factorizes into a part that depends directly on the γNN vertex and a part containing the nuclear structure dependence. The former is the single-nucleon tensor given by

$$\mathcal{W}^{\mu\nu}_{mm'}(\mathbf{p}, \mathbf{q}; S_N) = \langle \mathbf{p}_N, m_N(S_N)|\hat{\Gamma}^\mu|\mathbf{p}, m'(\xi)\rangle^* \langle \mathbf{p}_N, m_N(S_N)|\hat{\Gamma}^\nu|\mathbf{p}, m(\xi)\rangle \,, \tag{8}$$

where $|\mathbf{p}, m(\xi)\rangle$ represents an on-shell spinor state characterized by four-momentum $\overline{P}^\mu = \left(\overline{E} \equiv \sqrt{\mathbf{p}^2 + m_N^2}, \mathbf{p}\right)$ and spin four-vector ξ^μ, and $\hat{\Gamma}^\mu$ is the off-shell γNN vertex operator. The indices m, m' denote the spin projection ($\pm 1/2$) in the z direction of the bound nucleon in its rest frame. The latter term

$$M_{mm'}(\mathbf{p}, \mathbf{\Omega}^*) = \sum_{M_B} \langle J_B M_B | a_{\mathbf{p}m'} | J_A J_A(\mathbf{\Omega}^*)\rangle^* \langle J_B M_B | a_{\mathbf{p}m} | J_A J_A(\mathbf{\Omega}^*)\rangle \tag{9}$$

is the polarized density matrix in momentum space for the polarized target, assuming 100% polarization in the $\mathbf{\Omega}^*$ direction and a specific nuclear transition $J_A \to J_B$ (see refs. [26, 27, 28, 32] for details).

Introducing these results in the general expression (4) for the cross section we obtain

$$\frac{d\sigma}{d\Omega_e d\varepsilon' d\Omega_N} = K f_{rec}^{-1} \sum_{mm'} \sigma^{ep}_{mm'}(\mathbf{p}, \mathbf{q}; S_N) M_{mm'}(\mathbf{p}, \mathbf{\Omega}^*) \,, \tag{10}$$

where we have introduced the off-shell polarized electron-proton cross section, $\sigma^{ep}_{mm'}$, that can be decomposed into polarized single-nucleon response functions according to

$$\begin{aligned} \sigma^{ep}_{mm'}(\mathbf{p}, \mathbf{q}; S_N) &= \frac{2\alpha^2}{Q^4}\left(\frac{\varepsilon'}{\varepsilon}\right) \eta_{\mu\nu} \mathcal{W}^{\mu\nu}_{mm'}(\mathbf{p}, \mathbf{q}; S_N) \\ &= \sigma_M \left[\sum_\alpha v_\alpha \mathcal{R}^\alpha_{mm'}(\mathbf{p}, \mathbf{q}; S_N) + h \sum_{\alpha'} v_{\alpha'} \mathcal{R}^{\alpha'}_{mm'}(\mathbf{p}, \mathbf{q}; S_N)\right] \end{aligned} \tag{11}$$

with $\alpha = L, T, TL, TT$ referring to the electron-unpolarized responses and $\alpha' = T', TL'$ to the electron-polarized ones. The explicit expressions of the polarized single-nucleon responses as components of the single-nucleon tensor $\mathcal{W}^{\mu\nu}_{mm'}$ are given in [26]. It is also important to point out that the functions $\mathcal{R}^{\alpha(\alpha')}_{mm'}$ depend in general on both nucleonic polarization degrees of freedom, namely the spin projections of the struck nucleon on the laboratory z-axis, m, m',

and the ejected proton S_N^μ. The hadronic response functions in PWIA are then given simply by taking the combination

$$R^{\alpha(\alpha')} = \sum_{mm'} \mathcal{R}^{\alpha(\alpha')}_{mm'}(\mathbf{p},\mathbf{q};S_N) M_{mm'}(\mathbf{p},\mathbf{\Omega}^*)\,. \tag{12}$$

The polarized momentum distribution M can be analyzed by introducing its scalar $\overline{M}$ and vector $\widehat{\mathbf{M}}$ spin components, which are defined as follows [27, 28]

$$\overline{M}(\mathbf{p},\mathbf{\Omega}^*) = \mathrm{Tr}\left[M(\mathbf{p},\mathbf{\Omega}^*)\right] \tag{13}$$

$$\widehat{\mathbf{M}}(\mathbf{p},\mathbf{\Omega}^*) = \mathrm{Tr}\left[\boldsymbol{\sigma} M(\mathbf{p},\mathbf{\Omega}^*)\right]\,. \tag{14}$$

In this paper we first focus our attention on the single-nucleon part of the problem, generalizing our previous results for $A(\vec{e},e'\vec{p})$ and $\vec{A}(\vec{e},e'p)$ processes. Before entering into a detailed discussion of the single-nucleon aspect of the problem, it is important to point out that the target polarization dependence occurs in the vector as well as in the scalar components of the momentum distributions. The analysis of this dependence is further simplified by writing the density matrix in terms of different tensor polarization components: $M_{mm'} = \sum_I M^{(I)}_{mm'}$. As shown in [27] the scalar term $\overline{M}$ only gets contributions from even-rank tensors, while only odd-rank tensors contribute to $\widehat{\mathbf{M}}$. The totally unpolarized target situation corresponds to taking $I = 0$, thus, only the scalar density $\overline{M}$ occurs in this case.

2.2 The Single-Nucleon Tensor: General Remarks

Following closely the notation introduced in [26] in the case of $\vec{A}(\vec{e},e'p)$ reactions, here we develop the explicit expression for the appropriate single-nucleon tensor that enters in the analysis of $\vec{A}(\vec{e},e'\vec{p})$. Given a specific prescription for the off-shell vertex $\hat{\Gamma}^\mu$ (we will consider the standard ones introduced by de Forest [45]) and making use of trace techniques, the single-nucleon tensor reads

$$\mathcal{W}^{\mu\nu}_{mm'}(\mathbf{p},\mathbf{q};S_N) = \frac{1}{16M_N^2}\mathrm{Tr}\left[(\overline{\not{P}}+M_N)(\delta_{mm'}+\gamma_5\,\not{\xi}_{mm'})\gamma^0\hat{\Gamma}^{\mu\dagger}\gamma^0(\not{P}_N+M_N)(1+\gamma_5\,\not{S}_N)\hat{\Gamma}^\nu\right] \tag{15}$$

with the pseudovector matrix $\xi^\mu_{mm'} \equiv \langle \mathbf{p}, m'(\xi)|\gamma^\mu\gamma^5|\mathbf{p}, m(\xi)\rangle$ which reduces to the four-spin ξ^μ in the diagonal case $m = m'$. The tensor (15) can be split into a symmetric ($\mathcal{S}$) and an antisymmetric ($\mathcal{A}$) term under $\mu \leftrightarrow \nu$, according to the number (even or odd) of γ_5 matrices appearing in the trace. One can write in general

$$\mathcal{W}^{\mu\nu}_{mm'}(\mathbf{p},\mathbf{q};S_N) = \delta_{mm'}\left[\mathcal{S}^{\mu\nu} + i\mathcal{A}^{\mu\nu}(S_N)\right] + \mathcal{S}'^{\mu\nu}_{mm'}(S_N) + i\mathcal{A}'^{\mu\nu}_{mm'}\,, \tag{16}$$

where the dependence upon the outgoing nucleon spin has been explicitly indicated. Moreover, while $\mathcal{S}^{\mu\nu}$ and $\mathcal{A}^{\mu\nu}(S_N)$ are real, the tensors $\mathcal{A}'^{\mu\nu}_{mm'}$ and $\mathcal{S}'^{\mu\nu}_{mm'}(S_N)$ are real for diagonal components $m = m'$ and in general complex for off-diagonal terms.

The expression (16) contains the whole information on the polarization degrees of freedom of the problem and shows clearly the difference with the cases studied in refs. [26, 43]. So, for a scattering process off polarized targets, if the outgoing nucleon polarization is not measured, the only tensors involved are $\mathcal{S}^{\mu\nu}$ and $\mathcal{A}'^{\mu\nu}_{mm'}$: this corresponds to the analysis presented in [26]. On the contrary, for a process with an unpolarized target and polarized ejected nucleon, the single-nucleon tensor reduces to $\mathcal{S}^{\mu\nu} + i\mathcal{A}^{\mu\nu}(S_N)$, i.e., the whole dependence on the recoil nucleon spin is contained in the antisymmetric tensor, which means that only the electron-polarized hadronic responses $R^{T'}$ and $R^{TL'}$ depend upon the nucleon polarization. As known, this is a consequence of the PWIA assumption. In the totally unpolarized situation, only $\mathcal{S}^{\mu\nu}$ survives giving rise to the four electron-unpolarized responses R^α, $\alpha = L, T, TL, TT$. Finally, it is important to note that the symmetric term $\mathcal{S}'^{\mu\nu}_{mm'}(S_N)$ depends simultaneously on both the target and ejected nucleon polarizations and contributes to those responses which are only constructed from the symmetric tensor, i.e., the four electron-unpolarized ones. In this paper our main attention will be focused on these new contributions giving rise to "skewed" polarization, as shown below.

In order to evaluate the various components of $\mathcal{W}^{\mu\nu}_{mm'}(\mathbf{p}, \mathbf{q}; S_N)$ we make use of the spin precession technique developed in [26]. This method essentially amounts to first calculate the tensor

$$\begin{aligned}
\mathcal{W}^{\mu\nu}(\xi; S_N) &\equiv \mathcal{W}^{\mu\nu}(\theta_R, \phi_R; S_N) \\
&= \frac{1}{16M_N^2}\mathrm{Tr}\left[(\overline{\not{P}} + M_N)(1+\gamma_5 \not{\xi})\gamma^0\Gamma^{\mu\dagger}\gamma^0(\not{P}_N + M_N)(1+\gamma_5 \not{S}_N)\Gamma^\nu\right] \\
&\equiv \underbrace{\mathcal{S}^{\mu\nu} + \mathcal{S}'^{\mu\nu}(\theta_R, \phi_R; S_N)}_{\mathcal{S}^{\mu\nu}(\xi; S_N)} + i\underbrace{\left[\mathcal{A}^{\mu\nu}(S_N) + \mathcal{A}'^{\mu\nu}(\theta_R, \phi_R)\right]}_{\mathcal{A}^{\mu\nu}(\xi; S_N)}, \qquad (17)
\end{aligned}$$

where the angles (θ_R, ϕ_R) specify the spin direction of the hit nucleon (with respect to the quantization axis) in its rest frame. Obviously, when boosted to the laboratory frame, the four-spin ξ^μ precesses to the positive (θ_L, ϕ_L) direction (see [26] for details on how the connection is made). Following [26] and after evaluating the components of ξ^μ, one finds the relations:

$$\begin{aligned}
\mathcal{W}^{\mu\nu}_{++} &= \mathcal{S}^{\mu\nu} + \mathcal{S}'^{\mu\nu}(0,0;S_N) + i\left[\mathcal{A}^{\mu\nu}(S_N) + \mathcal{A}'^{\mu\nu}(0,0)\right] \\
\mathcal{W}^{\mu\nu}_{--} &= \mathcal{S}^{\mu\nu} - \mathcal{S}'^{\mu\nu}(0,0;S_N) + i\left[\mathcal{A}^{\mu\nu}(S_N) - \mathcal{A}'^{\mu\nu}(0,0)\right] \\
\mathcal{W}^{\mu\nu}_{+-} &= \mathcal{S}'^{\mu\nu}(\frac{\pi}{2}, 0; S_N) - \mathcal{A}'^{\mu\nu}(\frac{\pi}{2}, \frac{\pi}{2}) + i\left[\mathcal{A}'^{\mu\nu}(\frac{\pi}{2}, 0) + \mathcal{S}'^{\mu\nu}(\frac{\pi}{2}, \frac{\pi}{2}; S_N)\right] \\
\mathcal{W}^{\mu\nu}_{-+} &= \mathcal{S}'^{\mu\nu}(\frac{\pi}{2}, 0; S_N) + \mathcal{A}'^{\mu\nu}(\frac{\pi}{2}, \frac{\pi}{2}) + i\left[\mathcal{A}'^{\mu\nu}(\frac{\pi}{2}, 0) - \mathcal{S}'^{\mu\nu}(\frac{\pi}{2}, \frac{\pi}{2}; S_N)\right], \qquad (18)
\end{aligned}$$

where we have used the results $\mathcal{S}'^{\mu\nu}(\pi, 0; S_N) = -\mathcal{S}'^{\mu\nu}(0, 0; S_N)$ and $\mathcal{A}'^{\mu\nu}(\pi, 0) = -\mathcal{A}'^{\mu\nu}(0, 0)$.

The analysis further simplifies by defining a new basis in which the single-nucleon tensors are given in the form [27, 28]:

$$
\begin{aligned}
0 &: \frac{1}{2}\left[\mathcal{W}^{\mu\nu}_{++} + \mathcal{W}^{\mu\nu}_{--}\right] = \mathcal{S}^{\mu\nu} + i\mathcal{A}^{\mu\nu}(S_N) \\
z &: \frac{1}{2}\left[\mathcal{W}^{\mu\nu}_{++} - \mathcal{W}^{\mu\nu}_{--}\right] = \mathcal{S}'^{\mu\nu}(0,0;S_N) + i\mathcal{A}'^{\mu\nu}(0,0) \\
x &: \frac{1}{2}\left[\mathcal{W}^{\mu\nu}_{+-} + \mathcal{W}^{\mu\nu}_{-+}\right] = \mathcal{S}'^{\mu\nu}(\frac{\pi}{2},0,S_N) + i\mathcal{A}'^{\mu\nu}(\frac{\pi}{2},0) \\
y &: -\frac{i}{2}\left[\mathcal{W}^{\mu\nu}_{+-} - \mathcal{W}^{\mu\nu}_{-+}\right] = \mathcal{S}'^{\mu\nu}(\frac{\pi}{2},\frac{\pi}{2};S_N) + i\mathcal{A}'^{\mu\nu}(\frac{\pi}{2},\frac{\pi}{2})\,.
\end{aligned}
\tag{19}
$$

Note that z denotes the component along the transfer momentum $\mathbf{q}$, whereas x and y are the vector components in the perpendicular scattering plane.

The explicit calculation of the single-nucleon tensor $\mathcal{W}^{\mu\nu}(\xi;S_N)$ for the two common choices, CC1 and CC2, of the current operator is presented in Appendix A. Once the single-nucleon tensor is known, the various responses $\mathcal{R}^{\alpha(\alpha')}_{mm'}(\theta_R,\phi_R;S_N)$ are constructed directly by taking the appropriate components. In Appendix B we summarize the expressions of all the single-nucleon responses making use of the basis introduced in (19). Hence, by analogy with the polarized density and following [28], the single-nucleon spin dependent responses $\mathcal{R}^{\alpha(\alpha')}_{mm'}$ can be analyzed by introducing scalar $\overline{\mathcal{R}}^{\alpha}$, $\overline{\mathcal{R}}^{\alpha'}(S_N)$ and vector $\widehat{\boldsymbol{\mathcal{R}}}^{\alpha}(S_N)$, $\widehat{\boldsymbol{\mathcal{R}}}^{\alpha'}$ components. As usual, $\alpha = L, T, TL, TT$ and $\alpha' = T', TL'$. Note that the vector responses (given by the three components referred to the xyz frame) only enter when the target is polarized, whereas the scalar ones may contribute even if the target is unpolarized (zero rank tensor in the scalar momentum distribution). Moreover, the explicit dependence in the outgoing nucleon polarization only enters in the scalar responses $\overline{\mathcal{R}}^{\alpha'}(S_N)$, which give rise to the two polarized hadronic responses $R^{T'}$ and $R^{TL'}$ that contribute to $A(\vec{e},e'\vec{p})$ reactions, and in the vector terms $\widehat{\boldsymbol{\mathcal{R}}}^{\alpha}(S_N)$, which also require polarization of the target and only affect the electron-unpolarized responses R^L, R^T, R^{TL} and R^{TT}.

2.3 Skewing responses and asymmetries

The hadronic response functions (12) can be expressed as follows:

- Electron-unpolarized responses: R^{α} with $\alpha = L, T, TL, TT$

$$
R^{\alpha} = \overline{\mathcal{R}}^{\alpha}\overline{M}(\mathbf{p},\boldsymbol{\Omega}^*) + \widehat{\boldsymbol{\mathcal{R}}}^{\alpha}(S_N)\cdot\widehat{\mathbf{M}}(\mathbf{p},\boldsymbol{\Omega}^*)\,. \tag{20}
$$

- Electron-polarized responses: $R^{\alpha'}$ with $\alpha' = T', TL'$

$$
R^{\alpha'} = \overline{\mathcal{R}}^{\alpha'}(S_N)\overline{M}(\mathbf{p},\boldsymbol{\Omega}^*) + \widehat{\boldsymbol{\mathcal{R}}}^{\alpha'}\cdot\widehat{\mathbf{M}}(\mathbf{p},\boldsymbol{\Omega}^*)\,. \tag{21}
$$

From (20) and (21) it comes out that for reactions with unpolarized targets, only the two terms involving the scalar momentum distribution (for zero rank tensor) contribute. From these, the one in (20) refers to the fully unpolarized situation whereas that in (21) requires measuring the polarization of the ejected nucleon as well. In the case of polarized targets, the vector momentum distribution also enters. Note, however, that in the case of the four electron-unpolarized responses (20) such contribution only enters if the outgoing nucleon spin is also measured.

The expressions given by eqs. (20,21) constitute one of the basic outcomes of this work because they show in a very clear way how the polarization degrees of freedom get organized in the scattering process. Therefore, concerning the single-nucleon aspect of the problem, a crucial difference emerges in the electron-polarized and electron-unpolarized observables. In the former, the whole spin dependence can be decoupled into two separate single nucleon responses, each one depending exclusively on one of the nucleon spin variables, the outgoing nucleon or the target (bound nucleon). This result is in accordance with the form in which the four-spin variables enter in the antisymmetric tensor, i.e., $(\xi \pm S_N)^\mu$ (see Appendix A). The electron-unpolarized case clearly differs: here the whole spin dependence in $\widehat{\boldsymbol{\mathcal{R}}}^\alpha(S_N)$ comes from the symmetric tensor, where the four-spin vectors enter through their scalar product (i.e., $S_N \cdot \xi$), and involves the polarization of both the target and the emitted nucleon. Therefore, since results for the totally unpolarized and polarized recoil nucleon responses, $\overline{\mathcal{R}}^\alpha$ and $\overline{\mathcal{R}}^{\alpha'}(S_N)$, have been presented in [43], whereas the pure polarized target single-nucleon responses $\widehat{\boldsymbol{\mathcal{R}}}^{\alpha'}$ were studied in [26], the analysis in this work will be focused on the new responses $\widehat{\boldsymbol{\mathcal{R}}}^\alpha(S_N)$. Accordingly, in the following we restrict to the case of unpolarized electrons, for which only the Σ part of the general cross section (5) enters.

The differential cross section (10) for $\vec{A}(e, e'\vec{p})$ can be written in PWIA in the form

$$\frac{d\sigma}{d\Omega_e d\varepsilon' d\Omega_N} = \Sigma = K f_{rec}^{-1} \left[\overline{\sigma}^{ep} \overline{M}(\mathbf{p}, \boldsymbol{\Omega}^*) + \widehat{\boldsymbol{\sigma}}^{ep}(S_N) \cdot \widehat{\mathbf{M}}(\mathbf{p}, \boldsymbol{\Omega}^*) \right] , \tag{22}$$

where the scalar and vector single-nucleon cross sections

$$\overline{\sigma}^{ep} = \sigma_M \sum_\alpha v_\alpha \overline{\mathcal{R}}^\alpha \tag{23}$$

$$\widehat{\boldsymbol{\sigma}}^{ep}(S_N) = \sigma_M \sum_\alpha v_\alpha \widehat{\boldsymbol{\mathcal{R}}}^\alpha(S_N) \tag{24}$$

have been introduced in analogy with the single nucleon response functions.

In the next section we present predictions for the polarization asymmetries obtained from the difference of cross sections for opposite ejected nucleon spin directions (denoted by the three-vector $\mathbf{s}_N$) divided by their sum, for a selected target orientation:

$$A_{\mathbf{s}_N} = \frac{\Sigma(\mathbf{s}_N) - \Sigma(-\mathbf{s}_N)}{\Sigma(\mathbf{s}_N) + \Sigma(-\mathbf{s}_N)} . \tag{25}$$

Making use of (22) and taking into account that the whole dependence of $\widehat{\boldsymbol{\sigma}}^{ep}$ upon the ejected nucleon spin components is linear (see Appendix A), the polarization asymmetries can be computed as

$$A_{\mathbf{s}_N} = \frac{\widehat{\boldsymbol{\sigma}}^{ep}(\mathbf{s}_N) \cdot \widehat{\mathbf{M}}(\mathbf{p}, \boldsymbol{\Omega}^*)}{\overline{\sigma}^{ep}\overline{M}(\mathbf{p}, \boldsymbol{\Omega}^*)} \,. \tag{26}$$

Finally, to make connection with the concept of "skewed" recoil polarization, we provide a geometrical interpretation of the polarized momentum distribution by introducing the following vector field

$$\boldsymbol{\chi}(\mathbf{p}, \boldsymbol{\Omega}) \equiv \frac{\widehat{\mathbf{M}}(\mathbf{p}, \boldsymbol{\Omega}^*)}{\overline{M}(\mathbf{p}, \boldsymbol{\Omega}^*)}. \tag{27}$$

It can be shown that in the independent particle model, this is a unit vector, $|\boldsymbol{\chi}| = 1$, and that, semi-classically, it coincides with the local spin field in momentum space [31, 32, 39] (see an example in Appendix C for the particular case of the ^{39}K nucleus analyzed in the next section). Since the dependence of the cross section on the final spin direction, S_N^μ, is linear, one can write the i-th component ($i = x, y, z$) of the vector cross section in the general form

$$\widehat{\sigma}_i^{ep}(\mathbf{s}_N) = \widehat{\sigma}_{\mu i}^{ep} S_N^\mu \,, \tag{28}$$

where we have introduced the tensor components $\widehat{\sigma}_{\mu i}^{ep}$ of the "skewing" cross section. Note that the half-covariant form of this tensor, with a covariant index, μ, and a spatial one, i, reflects the fact that the target momentum distribution is being described within a non-relativistic framework. Hence the full covariance of the equations is broken at this level, since we do not provide a covariant description of the nuclear target.

Similarly to the vector cross-section, the asymmetry (26) can also be written as

$$A_{\mathbf{s}_N} = A_{\mu i} S_N^\mu \chi_i \,, \tag{29}$$

where a sum over the spatial index, i, is understood, and we have introduced the tensor asymmetry

$$A_{\mu i} = \frac{\widehat{\sigma}_{\mu i}^{ep}}{\overline{\sigma}^{ep}} \,. \tag{30}$$

Now for given kinematics and target polarization, we introduce the "skewed" four-vector $R^\mu = (r_0, \mathbf{r})$, defined as

$$R_\mu = -A_{\mu i} \chi_i \,. \tag{31}$$

The asymmetry can then be written as

$$A_{\mathbf{s}_N} = -R_\mu S_N^\mu = -r_0 \sqrt{\mathbf{s}_N^2 - 1} + \mathbf{r} \cdot \mathbf{s}_N \tag{32}$$

since S_N verifies $S_N^2 = -1$. For a fixed value of R^μ, the above asymmetry is maximum for $\mathbf{s}_N$ in the direction of $\mathbf{r}$ and $\mathbf{s}_N^2 = \mathbf{r}^2/(\mathbf{r}^2 - r_0^2)$. Therefore R^μ determines the preferred

polarization direction for the final proton: it is obtained as the linear transformation (31) of the local spin field (27), producing in this way the "skewing" effect we are referring to in this work.

3 Results for $\vec{A}(e, e'\vec{p})$

In this section we present results for the new "skewing" observables arising in $\vec{A}(e, e'\vec{p})$ reactions. Two kinematical settings already used in previous studies [26, 43] are considered. The former corresponds to quasi-perpendicular kinematics, where the values of the transfer momentum q and transfer energy ω are fixed. The values selected are $q = 500$ MeV/c and $\omega = 131.6$ MeV, which corresponds almost to the quasielastic peak center. The azimuthal angle of the recoil nucleon momentum is fixed to $\phi_N = 0^0$, i.e., coplanar kinematics. The second kinematics corresponds to parallel kinematics, where the outgoing nucleon momentum $\mathbf{p}_N$ is parallel to $\mathbf{q}$, i.e., $\theta_N = 0^o$. The kinetic energy of the recoil nucleon is fixed, as well as the electron beam energy.

Concerning the recoil nucleon polarization, we use the coordinate system defined by the axes $\mathbf{l}$ (parallel to $\mathbf{p}_N$), $\mathbf{n}$ (perpendicular to the plane containing $\mathbf{p}_N$ and $\mathbf{q}$) and $\mathbf{s}$ (determined by $\mathbf{n} \times \mathbf{l}$). This contrasts with the target polarization, which is referred to the (x, y, z) system with z given by the direction of $\mathbf{q}$. Hence, an important difference emerges when analyzing results corresponding to both kinematics. For the quasi-perpendicular case, varying the missing momentum means changing the direction in which the outgoing nucleon is detected. Hence the $\mathbf{l}$ and $\mathbf{s}$ directions which specify the recoil nucleon spin do not coincide with the components z, x used for the bound nucleon polarization components. On the contrary, the transverse direction $\mathbf{n}$ points along the y axis as far as coplanar, $\phi_N = 0^o$, kinematics is selected. Within the parallel situation, varying the missing momentum p implies changing the magnitude of q. In this case the system specified by $(\mathbf{l}, \mathbf{s}, \mathbf{n})$ coincides with (z, x, y). As will be shown, this leads to a cancellation of some responses and, moreover, symmetries in most of the scalar and vector single-nucleon responses emerge.

3.1 Single-nucleon responses

We start by showing the new vector polarized single-nucleon responses $\widehat{\boldsymbol{\mathcal{R}}}^{\alpha}(S_N)$ that enter in the analysis of $\vec{A}(e, e'\vec{p})$ reactions within PWIA. Following previous studies on $\vec{A}(\vec{e}, e'p)$ and $A(\vec{e}, e'\vec{p})$ processes [26, 43], here the off-shell character of the bound nucleon is explored making use of the current operator choice, CC1 vs CC2, and several prescriptions to restore current conservation, namely Coulomb, Landau and Weyl gauges (see [26, 41] for more details). The discrepancy among the various models of electromagnetic current allows one

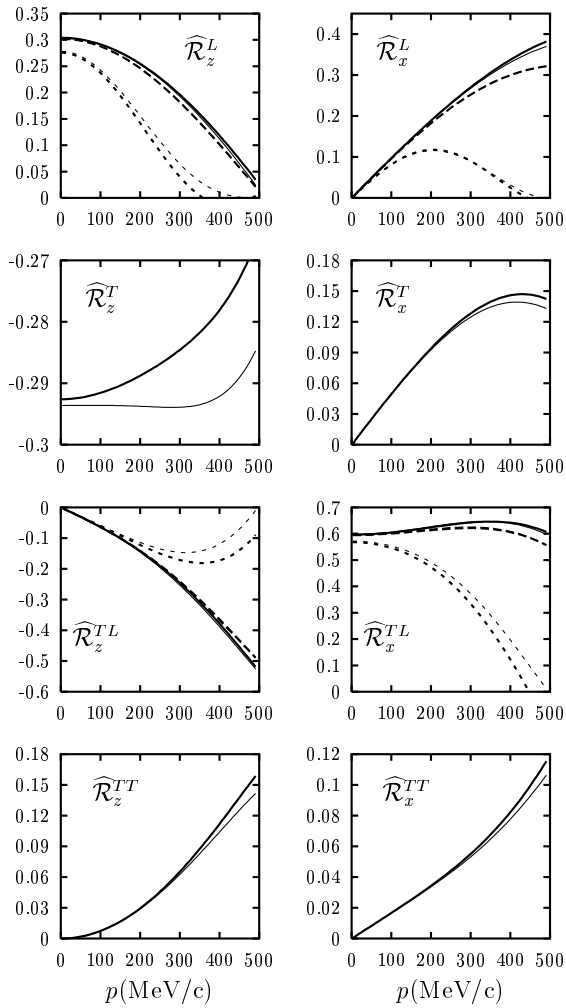

Figure 2: Electron-unpolarized vector single-nucleon responses $\widehat{\boldsymbol{\mathcal{R}}}^{\alpha}(S_N) = (\widehat{\mathcal{R}}_x^{\alpha}, \widehat{\mathcal{R}}_y^{\alpha}, \widehat{\mathcal{R}}_z^{\alpha})$ for quasi-perpendicular kinematics at momentum and energy transfer $q = 500$ MeV/c and $\omega = 131.6$ MeV, respectively. The outgoing nucleon polarization is along the longitudinal direction ($\mathbf{l}$). Thin lines correspond to the CC1 current operator and thick lines to the CC2 current. Results are shown for Landau (solid lines), Coulomb (dashed lines) and Weyl (short-dashed lines) gauges.

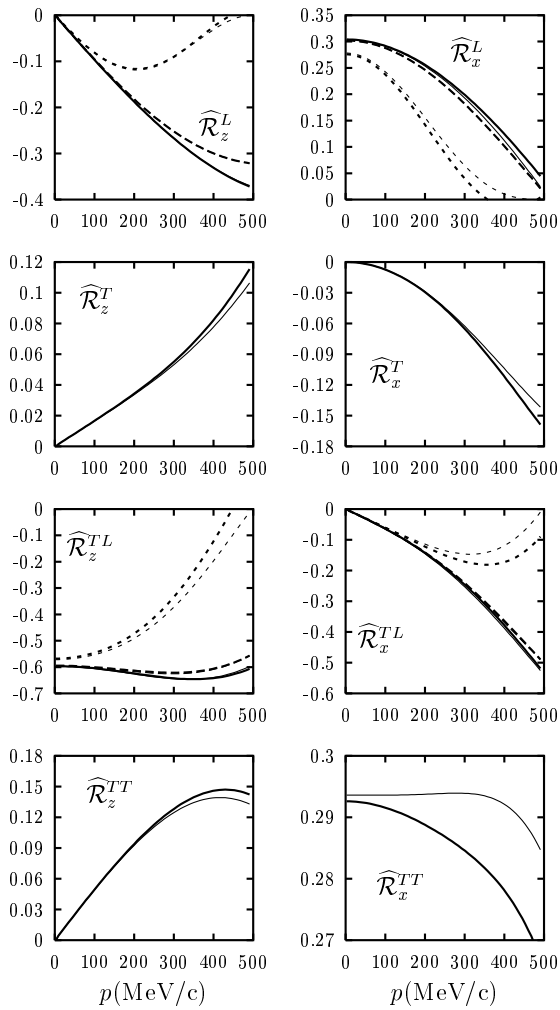

Figure 3: Same as fig. 2 but for the outgoing nucleon polarized along the sideways direction (**s**).

to get some insight into the importance of the off-shell effects on these observables.

Figures 2–4 show the components of the vector $\widehat{\boldsymbol{\mathcal{R}}}^{\alpha}(S_N)$ for quasi-perpendicular kinematics as functions of the missing momentum. Specifically, results in Fig. 2 correspond to longitudinal (**l**), Fig. 3 to sideways (**s**), and Fig. 4 to normal (**n**) recoil nucleon polarization. In the first two cases, the components $\widehat{\mathcal{R}}_y^{\alpha}$ are zero because of the azimuthal angle selected, $\phi_N = 0^o$. On the contrary, for outgoing polarization along **n** (Fig. 4), the only components which survive are $\widehat{\mathcal{R}}_y^{\alpha}$. Note that, as already mentioned, the **n** direction lies along the y axis for $\phi_N = 0^o$.

To begin the analysis we discuss the symmetries emerging from our results, by comparing

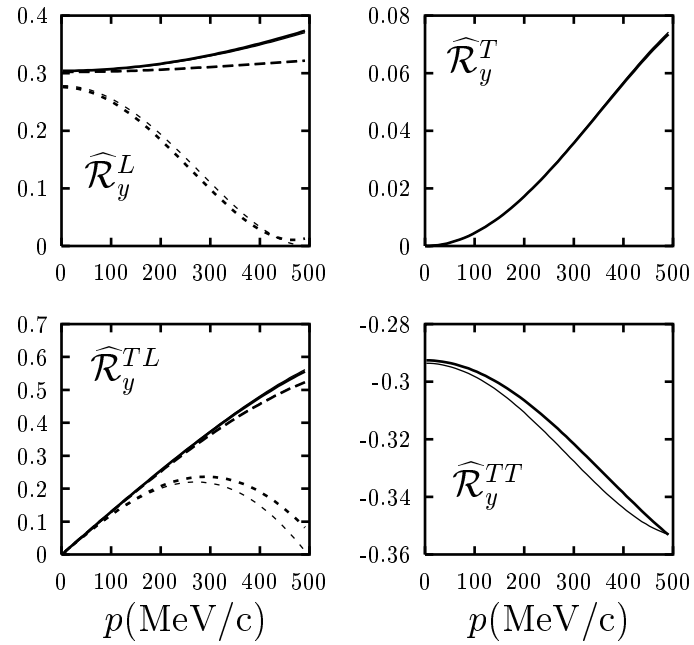

Figure 4: Same as fig. 2 but for the outgoing nucleon polarized along the normal direction ($\mathbf{n}$).

Figs. 2 and 3, i.e., recoil nucleon spin along $\mathbf{l}$ and $\mathbf{s}$, respectively. These symmetries are

$$\widehat{\mathcal{R}}_z^{L(TL)}(\mathbf{l}) = \widehat{\mathcal{R}}_x^{L(TL)}(\mathbf{s}) \quad ; \quad \widehat{\mathcal{R}}_x^{L(TL)}(\mathbf{l}) = -\widehat{\mathcal{R}}_z^{L(TL)}(\mathbf{s}) \tag{33}$$

$$\widehat{\mathcal{R}}_z^{T(TT)}(\mathbf{l}) = -\widehat{\mathcal{R}}_x^{TT(T)}(\mathbf{s}) \quad ; \quad \widehat{\mathcal{R}}_x^{T(TT)}(\mathbf{l}) = \widehat{\mathcal{R}}_z^{TT(T)}(\mathbf{s})\,. \tag{34}$$

Note the interchange between the two purely transverse responses. An analytical proof of the above symmetries can be provided within the non relativistic limit [46].

In the case of recoil nucleon spin along the normal direction, $\mathbf{n}$, the polarized single-nucleon responses shown in Fig. 4 result to be related to the scalar responses $\overline{\mathcal{R}}^{\alpha}$, corresponding to unpolarized recoil protons (see results in refs. [26, 43]). In fact the following identities hold for all the off-shell prescriptions:

$$\widehat{\mathcal{R}}_y^{L(TL)}(\mathbf{n}) = \overline{\mathcal{R}}^{L(TL)} \quad ; \quad \widehat{\mathcal{R}}_y^{T(TT)}(\mathbf{n}) = -\overline{\mathcal{R}}^{TT(T)}\,. \tag{35}$$

From these specific symmetries one could think that no new information could be obtained by measuring the nucleon polarization in these conditions. However note that the different role played by the T and TT responses would make this measurement an alternative way to separate the contributions of the different responses. As an example let us consider the case of a ^{39}K nucleus polarized in the y direction and described in a simple shell model (see section 3.2 and appendix C). In this situation and for coplanar kinematics, only the y

component of the vector momentum distribution survives. The single-nucleon contribution to the cross section (22) for $\mathbf{s}_N$ along the $\mathbf{n}$ direction is then given by

$$\overline{\sigma}^{ep} - \widehat{\sigma}_y^{ep}(\mathbf{n}) = (v_T + v_{TT})(\overline{\mathcal{R}}^T + \overline{\mathcal{R}}^{TT}) \,, \tag{36}$$

since the L and TL responses cancel out. This would allow to isolate the sum of the T and TT responses. In general, FSI are expected to break these symmetries at some level, since it is known that an additional normal polarization is induced even for unpolarized nuclei. However for intermediate values of the momentum transfer considered here ($q \simeq 500$ MeV/c) the polarization induced by FSI is expected to be small (≤ 0.2). This is indicated both by experimental data [11] and by calculations [19, 39].

Regarding the off-shell effects and gauge ambiguities in $\widehat{\boldsymbol{\mathcal{R}}}^{\alpha}(S_N)$, the discrepancies among the different prescriptions observed in Figs. 2-4 are similar to the ones already presented and discussed at length for the scalar $\overline{\mathcal{R}}^{\alpha}, \overline{\mathcal{R}}^{\alpha'}(S_N)$ and vector $\widehat{\boldsymbol{\mathcal{R}}}^{\alpha'}$ components [26, 43]. The basic findings may be summarized as follows. For those responses that involve the longitudinal component of the current, i.e., L and TL, the largest deviations are observed for the Weyl gauge (short-dashed lines). On the contrary, the four remaining off-shell prescriptions based on both current operators and the Coulomb and Landau gauges lead to similar results in all the cases. Gauge ambiguities do not affect the pure transverse responses T and TT, and the two current operator choices give rise to results which do not deviate significantly.

Results in parallel kinematics are presented in Fig. 5. As known, in this situation the usual directions that specify the recoil nucleon polarization $(\mathbf{l}, \mathbf{s}, \mathbf{n})$ coincide with the axes (z, x, y) used to characterize the bound nucleon (target) polarization. This leads to many symmetry relations among the various responses. Moreover, many components in the vector term $\widehat{\boldsymbol{\mathcal{R}}}^{\alpha}(S_N)$ vanish. Upper, middle and bottom rows in Fig. 5 correspond to longitudinal, sideways and normal ejected nucleon polarizations, respectively. From the total set of twelve $\widehat{\mathcal{R}}^{\alpha}_{x,y,z}$ components, only three survive for $\mathbf{l}$ and $\mathbf{s}$ polarization directions, and two in the case of normal $\mathbf{n}$. Furthermore, the symmetries among different single-nucleon responses, shown in eqs. (33–35), also apply to the results in parallel kinematics. Note that, in this particular situation, the only surviving responses are those which differ from zero in the $p \to 0$ limit for quasi-perpendicular kinematics. Obviously, the limit of missing momentum going to zero in (q, ω)-constant kinematics corresponds to $\theta_N \to 0$, i.e., approaching parallel kinematics. Finally, the two components for normal recoil nucleon polarization (bottom line) also satisfy the relations: $\widehat{\mathcal{R}}^L_y(\mathbf{n}) = \widehat{\mathcal{R}}^L_z(\mathbf{l}) = \widehat{\mathcal{R}}^L_x(\mathbf{s})$ and $\widehat{\mathcal{R}}^{TT}_y(\mathbf{n}) = \widehat{\mathcal{R}}^T_z(\mathbf{l}) = -\widehat{\mathcal{R}}^{TT}_x(\mathbf{s})$. Finally, although the two scalar responses that survive in parallel kinematics are not shown here, it is worth pointing out that they verify the relations $\overline{\mathcal{R}}^L = \widehat{\mathcal{R}}^L_y(\mathbf{n})$ and $\overline{\mathcal{R}}^T = -\widehat{\mathcal{R}}^{TT}_y(\mathbf{n})$. These symmetries are exactly fulfilled in all the off-shell prescriptions which, otherwise, lead to ambiguities of the same order as those discussed for quasi-perpendicular kinematics.

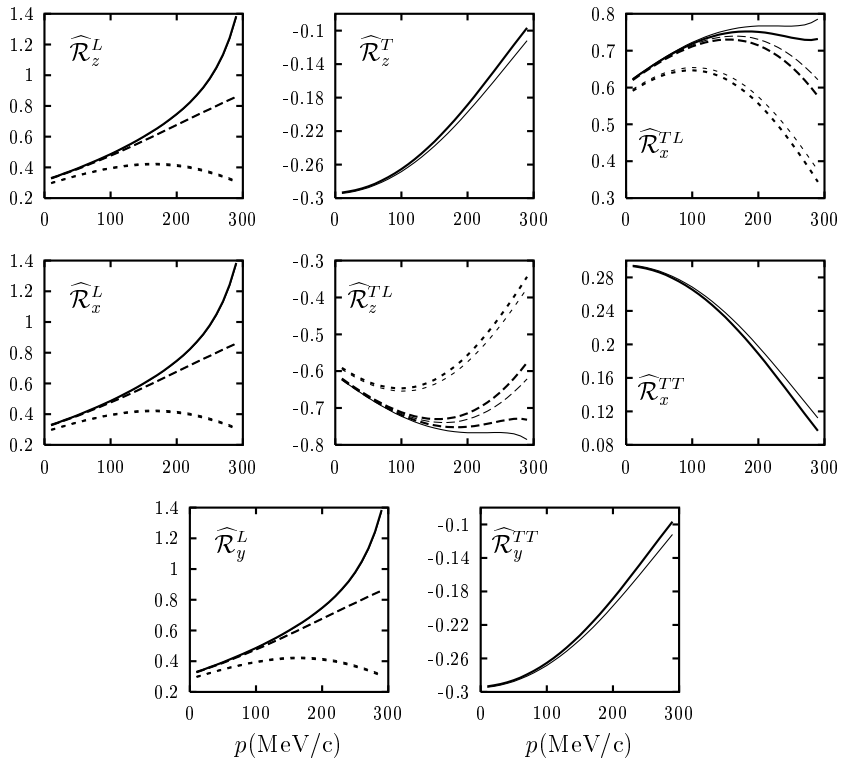

Figure 5: Same responses as in Fig. 2 but for parallel kinematics. Top, middle and bottom results correspond to the ejected nucleon polarized along the **l**, **s** and **n** directions, respectively. The value of the outgoing nucleon momentum is $p_N = 490$ MeV/c and the electron beam energy $\varepsilon = 500$ MeV.

3.2 Skewed polarization asymmetries

In the previous section we have shown the "skewing" single nucleon responses which are purely associated to the simultaneous measurement of target and ejected nucleon polarizations. In this section we explore polarized observables such as the cross sections and, more specifically, the polarization asymmetries introduced in (26).

The evaluation of the cross sections, within PWIA, requires not only the above discussed single-nucleon ingredients but also the polarized momentum distribution. Being aware of the crucial role of FSI upon cross sections and hadronic response functions, here we restrict our attention to polarization asymmetries. In fact ratios of two cross sections are expected to be much less sensitive to FSI effects. This is the case for transferred polarization asymmetries in $A(\vec{e}, e'\vec{p})$ reactions, where the PWIA results coincide for moderate missing momentum with much more elaborate relativistic distorted wave impulse approximation (RDWIA) calculations [24]. The same comment applies to the analysis of electron scattering on polarized targets [28, 31, 32, 39].

To analyze the polarization asymmetries we consider again the directions $\mathbf{l}, \mathbf{s}, \mathbf{n}$ for the ejected nucleon polarization, and target orientation selected along the axes x, y, z. A detailed study of the polarized momentum distribution for deformed nuclei has been presented in [27, 28]. The case of spherical nuclei within a shell model framework has been analyzed in [47] for inclusive $\vec{A}(\vec{e}, e')$ processes and in [30, 31, 32] for exclusive ones. Here we consider a simple model where the last bound nucleons are responsible for the spin of the polarized target. Specifically for ^{39}K, described as a hole nucleus with respect to the ^{40}Ca core, the orbit involved in the process is $d_{3/2}$. Since the target has spin $\frac{3}{2}$, the scalar polarized momentum distribution has even rank ($I = 0, 2$) components, while the vector term $\widehat{\mathbf{M}}$ odd rank ($I = 1, 3$) components. Only transitions leading to the residual nucleus ^{38}Ar in its ground state, described as two protons in the $d_{3/2}$ orbit coupled to total angular momentum $J_B = 0$, are considered.

In Figs. 6 and 7 we show the results for the polarization ratios (26) corresponding to quasi-perpendicular and parallel kinematics, respectively. To simplify the analysis, only the Coulomb gauge with the two current operator choices has been considered. Results for the Landau gauge are very similar, whereas those for the Weyl gauge deviate significantly for missing momentum values $p \geq 300$ MeV/c. For both kinematical situations, left panels correspond to forward electron scattering ($\theta_e = 30^o$), where the main contributions come from the longitudinal responses, and right panels to backward angles ($\theta_e = 150^o$), where the transverse responses dominate. In the case of (q, ω)-constant kinematics (Fig. 6) and target polarized along z and x (top and middle panels), only the longitudinal $\mathbf{l}$ and sideways $\mathbf{s}$ polarization asymmetries survive, whereas for the target orientation along y (bottom panels)

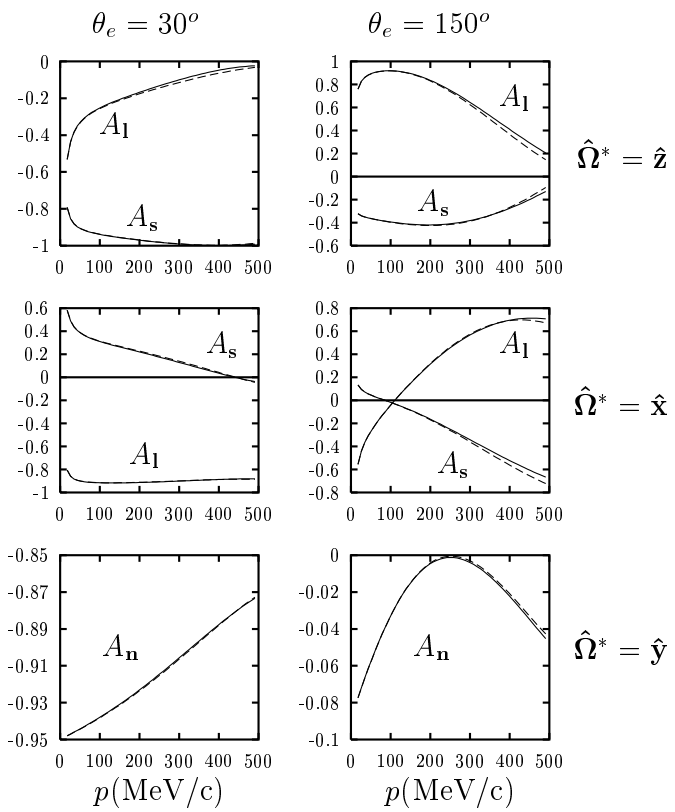

Figure 6: Polarization asymmetries $A_{\mathbf{l,s,n}}$ as defined in (26) for quasi-perpendicular kinematics. Results are presented for both current operators, $CC1$ (solid) and $CC2$ (dashed) in the Coulomb gauge.

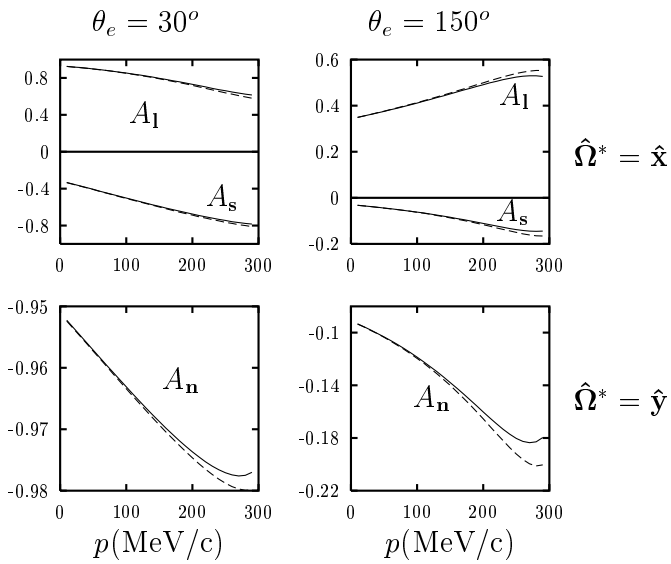

Figure 7: Same as Fig. 6 but for parallel kinematics. In this case the polarized momentum distribution does not enter for the target oriented along the z-axis.

only $A_{\mathbf{n}}$ differs from zero.

The above results can be easily understood by combining the single-nucleon responses shown in Figs. 2 and 3 with the general properties of the polarized momentum distribution, shown in Fig. 8 for the case of interest in this work, i.e., knockout from ^{39}K. The latter is displayed for the two kinematical settings and three orientations of the target polarization: along z, x and y. Note that for quasi-perpendicular kinematics (top panels of Fig. 8) the vector term $\widehat{\mathbf{M}}$ has no $\widehat{M}_y$ contribution for $\mathbf{\Omega}^*$ along z and x directions. On the contrary, for $\mathbf{\Omega}^*$ parallel to the y-axis, only the vector $\widehat{M}_y$ component survives and it is equal to $-\overline{M}$. This agrees with the general finding, shown in ref. [32], that $\left|\widehat{\mathbf{M}}\right| = \left|\overline{M}\right|$ (more details are given in Appendix C). In the case of parallel kinematics (bottom panels), the polarized momentum distribution does not contribute for target orientation along z. Note that in this case z coincides with the missing momentum direction. It is also important to point out that the scalar components $\overline{M}$, and consequently the non-vanishing vector ones, are identical for both target orientations.

Returning to the discussion of the polarization asymmetries, results in Figs. 6 and 7 show that target and ejected nucleon polarizations lead in general to very significant effects in the analysis of $\vec{A}(e, e'\vec{p})$ reactions. Specifically, large polarizations are found for some directions, reaching almost ± 1, and a clear separation between the longitudinal ($\mathbf{l}$) and sideways ($\mathbf{s}$) nucleon spin directions is present in all cases. Concerning Fig. 6, some specific symmetries, connected with the results obtained for the single-nucleon responses shown in previous sec-

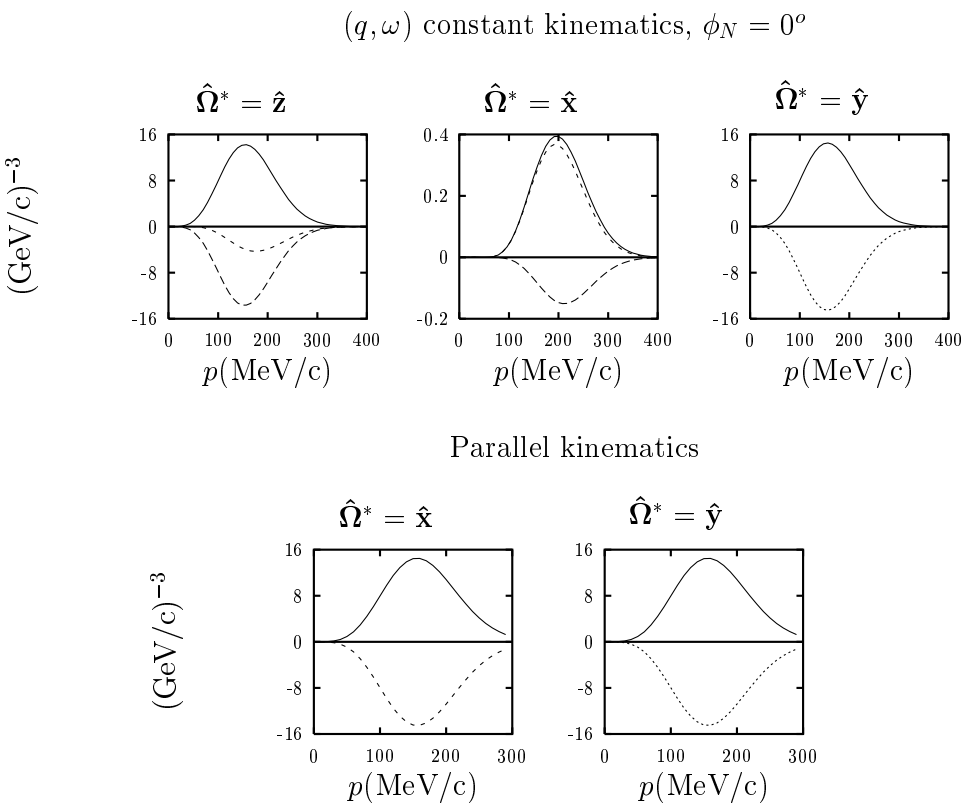

Figure 8: Scalar and vector polarized momentum distribution for proton knockout from ^{39}K leading to the residual nucleus in its ground state. The labelling of the curves is as follows: $\overline{M}$ (solid), $\widehat{M}_x$ (short-dashed), $\widehat{M}_y$ (dotted) and $\widehat{M}_z$ (dashed).

tion, also emerge. This is the situation for $\theta_e = 30^o$, where $A_{\mathbf{s}}$ ($A_{\mathbf{l}}$) for $\mathbf{\Omega}^*$ along z is shown to be very similar to $A_{\mathbf{l}}$ ($-A_{\mathbf{s}}$) for $\mathbf{\Omega}^*$ along x. This outcome does not appear for $\theta_e = 150^o$, where the symmetries of the dominant transverse responses involve the interchange of the T and TT components simultaneously —see (33–34). In the case of target polarization along y (bottom panels), the only non-vanishing vector component of the momentum distribution is $\widehat{M}_y$. Hence, the numerator in the polarization asymmetry arises from the single-nucleon cross section term $\widehat{\sigma}_y^{ep}$, which only enters for normal ($\mathbf{n}$) ejected nucleon polarization. Because of the general properties of the polarized momentum distribution, $A_{\mathbf{n}}$ does only depend on the single-nucleon cross section, being $A_{\mathbf{n}} = -\widehat{\sigma}_y^{ep}(\mathbf{n})/\overline{\sigma}^{ep}$. As shown, the absolute value of $A_{\mathbf{n}}$ is close to 1 for $\theta_e = 30^o$, being almost negligible for $\theta_e = 150^o$, where the dominant polarized transverse responses give a much smaller contribution (see results in previous section).

Next we consider the results for parallel kinematics (Fig. 7). Here only the target orientations along x and y directions contribute. In the former case (upper panel), the asymmetries $A_{\mathbf{l}}$ and $A_{\mathbf{s}}$ show significant effects and their specific contributions are clearly separated. This behaviour can be understood from results in section 3.1 and making use of the general properties of the polarized momentum distribution [27, 32]. Indeed one simply gets $A_{\mathbf{l}} = -\widehat{\sigma}_x^{ep}(\mathbf{l})/\overline{\sigma}^{ep}$ and $A_{\mathbf{s}} = -\widehat{\sigma}_x^{ep}(\mathbf{s})/\overline{\sigma}^{ep}$ for $\mathbf{\Omega}^*$ along x, and $A_{\mathbf{n}} = -\widehat{\sigma}_y^{ep}(\mathbf{n})/\overline{\sigma}^{ep}$ for $\mathbf{\Omega}^*$ in the y direction. As in Fig. 6, results corresponding to forward and backward electron scattering angles are very different, being the global contribution bigger in the former situation.

To conclude, we are aware of the inherent difficulties in performing double polarized experiments involving polarized target and ejected nucleon. However, the significant polarization effects shown in Figs. 6 and 7 are of interest as complementary information to the transferred polarization ratios $P'_{l,s}$ measured in $A(\vec{e}, e'\vec{p})$ processes, which have been proved to be almost insensitive to FSI [24]. This is likely to be also the case for the polarization ratios introduced in (26), since they survive in PWIA. Moreover, as previously discussed, the "skewed" polarization asymmetries (26) are proved to depend mostly (in some cases exclusively) on the single-nucleon content of the problem, and this is in accordance with the behaviour of $P'_{l,s}$ (see [24]). Therefore, the analysis of $A_{\mathbf{l},\mathbf{s},\mathbf{n}}(\mathbf{\Omega}^*)$ could also contribute to a better understanding of the properties of nucleons inside nuclei.

4 Conclusions

The main objective of this work has been to answer the question: "does the simultaneous measurement of target and ejected nucleon polarizations provide *significant* information which could improve our knowledge of electron scattering reactions?". Double-polarized $\vec{A}(e, e'\vec{p})$ experiments involve technical difficulties we are aware of; hence the physical moti-

vations for measuring specific observables need to be carefully explored and discussed. The present research represents a first step in this direction.

We have focused on the new observables arising as polarization transfer from the target to the ejected nucleon. These are different from the usual polarization transfer observables measured in $A(\vec{e}, e'\vec{p})$ reactions. To distinguish from these, we have introduced the term "skewed" polarization: it can be pictured as a twist of the spin of the hit nucleon inside the polarized target.

The analysis of "skewed" polarization in $\vec{A}(e, e'\vec{p})$ has been carried out within the framework of PWIA. Obviously, PWIA is too simple to provide realistic cross sections and response functions to be compared with the experiment. However, ratios of cross sections are expected to be much less sensitive to FSI effects than the cross sections themselves. This has been shown to be the case for the transferred polarization asymmetries $P'_{l,s}$, where PWIA predictions for missing momenta up to the Fermi momentum coincide with much more elaborated calculations involving relativistic and non-relativistic distorted wave approaches [19, 24]. Therefore, we are reasonably confident that our predictions for the polarization asymmetries introduced in (26) will be roughly valid within more sophisticated approximations.

A further merit of PWIA lies on the fact that, besides its simplicity, it allows to treat relativistic aspects of the reaction in a complete way. Moreover, polarization dependence in the general scattering problem also emerges within PWIA in a very clear way. So, the analysis presented in Section 2 contains some of the basic findings of this work. Specifically, the expressions given in (20,21) allow one to identify how spin degrees of freedom get organized in the different observables. A crucial difference comes out between the electron-polarized and electron-unpolarized responses. In the former, the whole dependence upon the spin goes simply as the sum of the bound and ejected nucleon four-spins, whereas for the latter, the product of four-spins is involved. Obviously, the scalar and vector momentum distributions, both dependent in general on the target polarization, must be also added in order to get final observables.

In presenting results for the new quantities needed to describe the process, we have first analyzed the "skewing" single-nucleon response functions for different off-shell prescriptions of the electromagnetic current. Second, we have presented predictions for the polarization asymmetries associated to a polarized ^{39}K target. The preliminary study performed in the present work indicates that experiments with simultaneously polarized target and recoil nucleon can provide additional information to that obtained from the separate investigation of $\vec{A}(\vec{e}, e'p)$ and $A(\vec{e}, e'\vec{p})$ processes. The predictions presented here for the asymmetries $A_{\mathbf{l,s,n}}(\mathbf{\Omega}^*)$, setting the scale of values expected for these new observables, constitute a promising starting point. Moreover, the strong dependence of the above asymmetries on the single-nucleon ingredients makes these observables suited to investigate nucleon properties,

complementing the analysis of transferred polarization ratios $P'_{l,s}$.

Acknowledgements

This work was partially supported by funds provided by DGI (Spain) and FEDER funds, under Contracts Nos. BFM2002-03218, BFM2002-03315 and FPA2002-04181-C04-04 and by the Junta de Andalucía, and by the INFN-CICYT collaboration agreement (project "Study of relativistic dynamics in electron and neutrino scattering").

Appendix A

We summarize the results for the single-nucleon tensors. For the two off-shell vertices we find the following. For the CC1 case:

$$
\begin{aligned}
4M_N^2\mathcal{S}^{\mu\nu}(\xi,S_N) &= G_M^2\Bigg[(1-\xi\cdot S_N)(\overline{P}^\mu P_N^\nu+\overline{P}^\nu P_N^\mu)+\frac{\overline{Q}^2}{2}g^{\mu\nu}(1-\xi\cdot S_N)\\
+\quad & P_N\cdot\xi(\overline{P}^\mu S_N^\nu+\overline{P}^\nu S_N^\mu)+\overline{P}\cdot S_N(P_N^\mu\xi^\nu+P_N^\nu\xi^\mu-g^{\mu\nu}P_N\cdot\xi)+\frac{\overline{Q}^2}{2}(\xi^\mu S_N^\nu+\xi^\nu S_N^\mu)\Bigg]\\
-\quad & \frac{F_2}{2}G_M\left[\overline{P}\cdot S_N(\xi^\mu R^\nu+\xi^\nu R^\mu)+P_N\cdot\xi(S_N^\mu R^\nu+S_N^\nu R^\mu)+2(1-\xi\cdot S_N)R^\mu R^\nu\right]\\
+\quad & \frac{F_2^2}{4M_N^2}R^\mu R^\nu\left[\overline{P}\cdot S_N P_N\cdot\xi+\left(2M_N^2-\frac{\overline{Q}^2}{2}\right)(1-\xi\cdot S_N)\right],
\end{aligned}
\tag{37}
$$

$$
\begin{aligned}
4M_N^2\mathcal{A}^{\mu\nu}(\xi,S_N) &= M_N^2G_M^2\epsilon^{\mu\nu\sigma\alpha}(\xi+S_N)_\sigma\overline{Q}_\alpha\\
+\quad & \frac{F_2}{2M_N}G_M(R^\mu\epsilon^{\sigma\alpha\beta\nu}-R^\nu\epsilon^{\sigma\alpha\beta\mu})(\xi+S_N)_\sigma\overline{P}_\alpha P_{N\beta}\,,
\end{aligned}
\tag{38}
$$

where $R^\mu\equiv(\overline{P}+P_N)^\mu$ and $\overline{Q}^\mu\equiv(P_N-\overline{P})^\mu$.

For the CC2 case, we have

$$
\begin{aligned}
4M_N^2\mathcal{S}^{\mu\nu}(\xi,S_N) &= F_1^2\Bigg[(1-\xi\cdot S_N)\left(\overline{P}^\mu P_N^\nu+\overline{P}^\nu P_N^\mu+\frac{\overline{Q}^2}{2}g^{\mu\nu}\right)+\frac{\overline{Q}^2}{2}(\xi^\mu S_N^\nu+\xi^\nu S_N^\mu)\\
+\quad & P_N\cdot\xi(\overline{P}^\mu S_N^\nu+\overline{P}^\nu S_N^\mu)+\overline{P}\cdot S_N(P_N^\mu\xi^\nu+P_N^\nu\xi^\mu)-g^{\mu\nu}P_N\cdot\xi\overline{P}\cdot S_N)\Bigg]\\
+\quad & \frac{F_1F_2}{2}\Big[2Q\cdot\overline{Q}(\xi^\mu S_N^\nu+\xi^\nu S_N^\mu)-(1-\xi\cdot S_N)(\overline{Q}^\mu Q^\nu+\overline{Q}^\nu Q^\mu-2g^{\mu\nu}Q\cdot\overline{Q})\\
+\quad & 2Q\cdot\xi(\overline{P}^\mu S_N^\nu+\overline{P}^\nu S_N^\mu-g^{\mu\nu}\overline{P}\cdot S_N)-2Q\cdot S_N(P_N^\mu\xi^\nu+P_N^\nu\xi^\mu-g^{\mu\nu}P_N\cdot\xi)
\end{aligned}
$$

$$
\begin{aligned}
&+ \quad \overline{P}\cdot S_N(\xi^\mu Q^\nu + \xi^\nu Q^\mu) - P_N\cdot\xi(S_N^\mu Q^\nu + S_N^\nu Q^\mu)\Big] \\
&+ \quad \frac{F_2^2}{4M_N^2}\Big[(Q\cdot S_N P_N\cdot\xi + Q\cdot P_N(1-\xi\cdot S_N))\,(\overline{P}^\mu Q^\nu + \overline{P}^\nu Q^\mu) \\
&+ \quad \Big(\overline{P}\cdot S_N Q\cdot\xi + \overline{P}\cdot Q(1-\xi\cdot S_N)\Big)\,(P_N^\mu Q^\nu + P_N^\nu Q^\mu) \\
&- \quad \Big(Q^2(1-\xi\cdot S_N) + 2Q\cdot\xi Q\cdot S_N\Big)\,(\overline{P}^\mu P_N^\nu + \overline{P}^\nu P_N^\mu) \\
&- \quad (Q^2 P_N\cdot\xi - 2Q\cdot\xi Q\cdot P_N)(\overline{P}^\mu S_N^\nu + \overline{P}^\nu S_N^\mu) \\
&- \quad (Q^2\overline{P}\cdot S_N - 2Q\cdot P_N Q\cdot S_N)(P_N^\mu\xi^\nu + P_N^\nu\xi^\mu) \\
&+ \quad \left(Q^2(2M_N^2 - \frac{\overline{Q}^2}{2}) - 2Q\cdot P_N Q\cdot\overline{P}\right)(\xi^\mu S_N^\nu + \xi^\nu S_N^\mu - g^{\mu\nu}\xi\cdot S_N) \\
&- \quad \left(Q\cdot S_N(2M_N^2 - \frac{\overline{Q}^2}{2}) - \overline{P}\cdot S_N Q\cdot P_N\right)(\xi^\mu Q^\nu + \xi^\nu Q^\mu - g^{\mu\nu}Q\cdot\xi) \\
&- \quad \left(Q\cdot\xi(2M_N^2 - \frac{\overline{Q}^2}{2}) - P_N\cdot\xi Q\cdot\overline{P}\right)(S_N^\mu Q^\nu + S_N^\nu Q^\mu - g^{\mu\nu}Q\cdot S_N) \\
&- \quad \left((1-\xi\cdot S_N)(2M_N^2 - \frac{\overline{Q}^2}{2}) + P_N\cdot\xi\overline{P}\cdot S_N\right)Q^\mu Q^\nu \\
&+ \quad g^{\mu\nu}\Bigg(Q^2(2M_N^2 - \frac{\overline{Q}^2}{2} + \overline{P}\cdot S_N P_N\cdot\xi) \\
&- \quad Q\cdot P_N(Q\cdot\overline{P} + Q\cdot\xi\overline{P}\cdot S_N) - Q\cdot\overline{P}(Q\cdot P_N + Q\cdot S_N P_N\cdot\xi)\Big)\Big]\,, \qquad (39)
\end{aligned}
$$

where $Q^\mu \equiv K^\mu - K'^\mu$ is the four-momentum transferred in the process. Finally

$$
\begin{aligned}
& 4M_N^2\mathcal{A}^{\mu\nu}(\xi, S_N) = M_N F_1^2\epsilon^{\alpha\beta\mu\nu}(\xi + S_N)_\alpha\overline{Q}_\beta \\
&+ \quad \frac{F_1F_2}{2M_N}\Big[\epsilon^{\alpha\beta\mu\nu}(2P_N\cdot Q\overline{P}_\alpha\xi_\beta + 2\overline{P}\cdot QP_{N\alpha}S_{N\beta}) \\
&+ \quad 2M_N^2\epsilon^{\alpha\beta\mu\nu}(\xi + S_N)_\alpha Q_\beta \\
&+ \quad (Q^\mu\epsilon^{\alpha\beta\gamma\nu} - Q^\nu\epsilon^{\alpha\beta\gamma\mu})(S_N - \xi)_\alpha P_{N\beta}\overline{P}_\gamma\Big] \\
&+ \quad \frac{F_2^2}{4M_N}\Big[\epsilon^{\alpha\beta\mu\nu}(2P_N\cdot Q\xi_\alpha Q_\beta - 2\overline{P}\cdot QS_{N\alpha}Q_\beta) + Q^2\epsilon^{\alpha\beta\mu\nu}(\overline{P} + P_N)_\alpha(\xi - S_N)_\beta \\
&+ \quad (Q^\mu\epsilon^{\alpha\beta\gamma\nu} - Q^\nu\epsilon^{\alpha\beta\gamma\mu})(\xi - S_N)_\alpha(\overline{P} + P_N)_\beta Q_\gamma\Big]\,. \qquad (40)
\end{aligned}
$$

Appendix B

In this appendix we show the explicit expressions of the scalar and vector single-nucleon responses by taking the appropriate components of the general tensor $\mathcal{W}^{\mu\nu}(\theta_R, \phi_R; S_N)$ as introduced in (17). To make clear the analysis, we fix the following notation: $\widehat{\boldsymbol{\mathcal{R}}}^{\alpha(\alpha')} \equiv$

$\left(\widehat{\mathcal{R}}_x^{\alpha(\alpha')}, \widehat{\mathcal{R}}_y^{\alpha(\alpha')}, \widehat{\mathcal{R}}_z^{\alpha(\alpha')}\right)$ for the three vector components, and $\overline{\mathcal{R}}^{\alpha(\alpha')}$ the scalar one. In terms of the tensor components given by the Lorentz indices μ, ν, referred to the $1-2-3$ hadron-plane-system of axes, the final expressions result:

- *Electron-unpolarized responses*

$$\begin{aligned}
\overline{\mathcal{R}}^L &= \mathcal{S}^{00} \\
\widehat{\mathcal{R}}_z^L &= \mathcal{S}'^{00}(0,0,S_N) \\
\widehat{\mathcal{R}}_x^L &= \mathcal{S}'^{00}(\frac{\pi}{2},0,S_N) \\
\widehat{\mathcal{R}}_y^L &= \mathcal{S}'^{00}(\frac{\pi}{2},\frac{\pi}{2},S_N)\,.
\end{aligned} \tag{41}$$

$$\begin{aligned}
\overline{\mathcal{R}}^T &= \mathcal{S}^{11} + \mathcal{S}^{22} \\
\widehat{\mathcal{R}}_z^T &= \mathcal{S}'^{11}(0,0,S_N) + \mathcal{S}'^{22}(0,0,S_N) \\
\widehat{\mathcal{R}}_x^T &= \mathcal{S}'^{11}(\pi/2,0,S_N) + \mathcal{S}'^{22}(\pi/2,0,S_N) \\
\widehat{\mathcal{R}}_y^T &= \mathcal{S}'^{11}(\pi/2,\pi/2,S_N) + \mathcal{S}'^{22}(\pi/2,\pi/2,S_N)\,.
\end{aligned} \tag{42}$$

$$\begin{aligned}
\overline{\mathcal{R}}^{TT} &= \left(\mathcal{S}^{22} - \mathcal{S}^{11}\right)\cos 2\phi_N \\
\widehat{\mathcal{R}}_z^{TT} &= \left[\mathcal{S}'^{22}(0,0,S_N) - \mathcal{S}'^{11}(0,0,S_N)\right]\cos 2\phi_N + 2\mathcal{S}'^{12}(0,0,S_N)\sin 2\phi_N \\
\widehat{\mathcal{R}}_x^{TT} &= \left[\mathcal{S}'^{22}(\pi/2,0,S_N) - \mathcal{S}'^{11}(\pi/2,0,S_N)\right]\cos 2\phi_N + 2\mathcal{S}'^{12}(\pi/2,0,S_N)\sin 2\phi_N \\
\widehat{\mathcal{R}}_y^{TT} &= \left[\mathcal{S}'^{22}(\pi/2,\pi/2,S_N) - \mathcal{S}'^{11}(\pi/2,\pi/2,S_N)\right]\cos 2\phi_N + 2\mathcal{S}'^{12}(\pi/2,\pi/2,S_N)\sin 2\phi_N\,.
\end{aligned} \tag{43}$$

$$\begin{aligned}
\overline{\mathcal{R}}^{TL} &= 2\sqrt{2}\mathcal{S}^{01}\cos\phi_N \\
\widehat{\mathcal{R}}_z^{TL} &= 2\sqrt{2}\left[\mathcal{S}'^{01}(0,0,S_N)\cos\phi_N - \mathcal{S}'^{02}(0,0,S_N)\sin\phi_N\right] \\
\widehat{\mathcal{R}}_x^{TL} &= 2\sqrt{2}\left[\mathcal{S}'^{01}(\pi/2,0,S_N)\cos\phi_N - \mathcal{S}'^{02}(\pi/2,0,S_N)\sin\phi_N\right] \\
\widehat{\mathcal{R}}_y^{TL} &= 2\sqrt{2}\left[\mathcal{S}'^{01}(\pi/2,\pi/2,S_N)\cos\phi_N - \mathcal{S}'^{02}(\pi/2,\pi/2,S_N)\sin\phi_N\right]\,.
\end{aligned} \tag{44}$$

- *Electron-polarized responses*

$$\begin{aligned}
\overline{\mathcal{R}}^{T'} &= -2\mathcal{A}^{12}(S_N) \\
\widehat{\mathcal{R}}_z^{T'} &= -2\mathcal{A}'^{12}(0,0) \\
\widehat{\mathcal{R}}_x^{T'} &= -2\mathcal{A}'^{12}(\pi/2,0) \\
\widehat{\mathcal{R}}_y^{T'} &= -2\mathcal{A}'^{12}(\pi/2,\pi/2)\,.
\end{aligned} \tag{45}$$

$$
\begin{aligned}
\overline{\mathcal{R}}^{TL'} &= -2\sqrt{2}\left[\mathcal{A}^{01}(S_N)\sin\phi_N + \mathcal{A}^{02}(S_N)\cos\phi_N\right] \\
\widehat{\mathcal{R}}_z^{TL'} &= -2\sqrt{2}\left[\mathcal{A}'^{01}(0,0)\sin\phi_N + \mathcal{A}'^{02}(0,0)\cos\phi_N\right] \\
\widehat{\mathcal{R}}_x^{TL'} &= -2\sqrt{2}\left[\mathcal{A}'^{01}(\pi/2,0)\sin\phi_N + \mathcal{A}'^{02}(\pi/2,0)\cos\phi_N\right] \\
\widehat{\mathcal{R}}_y^{TL'} &= -2\sqrt{2}\left[\mathcal{A}'^{01}(\pi/2,\pi/2)\sin\phi_N + \mathcal{A}'^{02}(\pi/2,\pi/2)\cos\phi_N\right] .
\end{aligned} \tag{46}
$$

Appendix C

In this Appendix we discuss in detail the geometrical interpretation of the polarized momentum distribution. In the case of interest in this work, a proton knocked out from the $d_{3/2}$ shell of ^{39}K and the daughter nucleus in its ground state, $J_B = 0$, the vector field $\boldsymbol{\chi}$ introduced in (27) reduces to

$$
\boldsymbol{\chi} = 2\frac{\boldsymbol{\Omega}^* \cdot \mathbf{p}}{p^2}\mathbf{p} - \boldsymbol{\Omega}^* . \tag{47}
$$

The symmetries of the momentum distribution can then be explained by taking specific directions of the target polarization $\boldsymbol{\Omega}^*$:

- $\boldsymbol{\Omega}^* = \hat{\mathbf{z}}$. In this case the nucleus is polarized along $\mathbf{q}$. For quasi-elastic kinematics $p_N \simeq q$, hence we can write $\cos\theta \simeq -\frac{p}{2q}$, where θ is the angle between $\mathbf{p}$ and $\mathbf{q}$. Therefore

$$
\boldsymbol{\chi} = -\frac{\mathbf{p}+\mathbf{q}}{q} . \tag{48}
$$

  For low values of the missing momentum (compared with q) we can also write $\sin\theta \simeq 1$ to leading order in p/q. The components of $\boldsymbol{\chi}$ are then

$$
\chi_x = -\frac{p_x}{q} \simeq -\frac{p}{q}, \qquad \chi_y = 0, \qquad \chi_z = -\frac{p_z}{q} - 1 \simeq -1 . \tag{49}
$$

  Therefore the following relations between vector and scalar momentum distributions

$$
\widehat{M}_x \simeq -\left(\frac{p}{q}\right)\overline{M}, \qquad \widehat{M}_y = 0, \qquad \widehat{M}_z \simeq -\overline{M}, \tag{50}
$$

  hold, in accord with the results of the upper-left panel of Fig. 8.

- $\boldsymbol{\Omega}^* = \hat{\mathbf{x}}$. In this case $\mathbf{p}\cdot\boldsymbol{\Omega}^* = p_x \simeq p$ and the field $\boldsymbol{\chi}$ is

$$
\boldsymbol{\chi} \simeq 2\frac{\mathbf{p}}{p} - \hat{\mathbf{x}}. \tag{51}
$$

  Hence we find to first order in p/q

$$
\chi_x = 2\frac{p_x}{p} - 1 \simeq 1, \qquad \chi_y = 0, \qquad \chi_z = 2\frac{p_z}{p} \simeq -\frac{p}{q} \tag{52}
$$

and for the momentum distribution components

$$\widehat{M}_x \simeq \overline{M}, \qquad \widehat{M}_y = 0, \qquad \widehat{M}_z \simeq -\frac{p}{q}\overline{M}, \tag{53}$$

explaining the results of the upper-middle panel of Fig. 8.

- $\mathbf{\Omega}^* = \hat{\mathbf{y}}$. In this case $\mathbf{p}$ is perpendicular to $\mathbf{\Omega}^*$, so $\boldsymbol{\chi} = -\hat{\mathbf{y}}$. Hence

$$\widehat{M}_x = \widehat{M}_z = 0, \qquad \widehat{M}_y = -\overline{M}, \tag{54}$$

giving the results of the upper-right panel of Fig. 8.

A similar analysis can be applied to the results for parallel kinematics (bottom panels of Fig. 8).

References

[1] S. Frullani and J. Mougey, Adv. Nucl. Phys. **14** (1985).

[2] A.S. Raskin, T.W. Donnelly, Ann. Phys. **191** (1989) 78.

[3] J. J. Kelly, Adv. Nucl. Phys. **23** (1996) 75.

[4] S. Boffi, C. Giusti, F. D. Pacati, M. Radici, *Electromagnetic response of atomic nuclei*, Oxford University Press (1996).

[5] T. W. Donnelly, M. J. Musolf, W. M. Alberico, M. B. Barbaro, A. De Pace and A. Molinari, Nucl. Phys. A **541** (1992) 525.

[6] M. J. Musolf, T. W. Donnelly, J. Dubach, S. J. . Pollock, S. Kowalski and E. J. Beise, Phys. Rept. **239** (1994) 1.

[7] W. M. Alberico, M. B. Barbaro, A. De Pace, T. W. Donnelly and A. Molinari, Nucl. Phys. A **563** (1993) 605.

[8] M. B. Barbaro, A. De Pace, T. W. Donnelly and A. Molinari, Nucl. Phys. A **569** (1994) 701.

[9] M. B. Barbaro, A. De Pace, T. W. Donnelly and A. Molinari, Nucl. Phys. A **596** (1996) 553.

[10] M. B. Barbaro, A. De Pace, T. W. Donnelly and A. Molinari, Nucl. Phys. A **598** (1996) 503.

[11] R.J. Woo et al., Phys. Rev. Lett. **80** (1998) 456.

[12] TJNAF proposal 89-033, C. Glashausser contact person.

[13] J.M. Udías, J.R. Vignote, Phys. Rev. **C62** (2000) 034302.

[14] H. Ito, S.E. Koonin, R. Seki, Phys. Rev. C **56** 3231 (1997).

[15] J. Ryckebusch, D. Debruyne, W. Van Nespen, and S. Janssen, Phys. Rev. C **60** 034604 (1999).

[16] J.J. Kelly, Phys. Rev. C **59** 3256 (1999).

[17] J.J. Kelly, Phys. Rev. C **60** 044609 (1999).

[18] J.I. Johanson and H.S. Sherif, Phys. Rev. C **59** 3481 (1999).

[19] F. Kazemi Tabatabaei, J.E. Amaro, J.A. Caballero, Phys. Rev. **C69** (2004) 064607.

[20] S. Malov, PhD thesis, New Brunswick, New Jersey, (1999), unpublished.

[21] S. Malov et al., Phys. Rev. **C62** (2000) 057302.

[22] S. Dieterich et al., Phys. Lett. **B500** (2001) 47.

[23] S. Strauch et al., Phys. Rev. Lett. **91** (2003) 052301.

[24] M.C. Martínez, J.R. Vignote, J.A. Caballero, T.W. Donnelly, E. Moya de Guerra, J.M. Udías, Phys. Rev. **C69** (2004) 034604.

[25] S. Boffi, C. Giusti, F.D. Pacati, Nucl. Phys. **A476** (1988) 617.

[26] J.A. Caballero, T.W. Donnelly, G.I. Poulis, Nucl. Phys. **A555** (1993) 709.

[27] J.A. Caballero, T.W. Donnelly, G.I. Poulis, E. Garrido, E. Moya de Guerra, Nucl. Phys. **A577** (1994) 528.

[28] E. Garrido, J.A. Caballero, E. Moya de Guerra, P. Sarriguren, J.M. Udías, Nucl. Phys. **A584** (1995) 256.

[29] J.A. Caballero, E. Garrido, E. Moya de Guerra, P. Sarriguren, J.M. Udías, Ann. Phys. **239** (1995) 351.

[30] J.E. Amaro and T.W. Donnelly, Ann. Phys. (N.Y.) **263** 56 (1998).

[31] J.E. Amaro, T.W. Donnelly, Nucl. Phys. **A 646** (1999) 187.

[32] J.E. Amaro, T.W. Donnelly, Nucl. Phys. **A 703** (2002) 541.

[33] H. Arenhövel, W. Leidemann and E.L. Tomusiak, nucl-th/0407053.

[34] H. Arenhövel, W. Leidemann and E.L. Tomusiak, Eur. Phys. Jou. **A** (2002) 491.

[35] H. Arenhövel, W. Leidemann and E.L. Tomusiak, Few Body Syst. 28 (2000) 147.

[36] H. Arenhövel, W. Leidemann and E.L. Tomusiak, Nucl. Phys. **A641** (1998) 517.

[37] H. Arenhövel, W. Leidemann and E.L. Tomusiak, Phys. Rev. C 52 (1995) 1232.

[38] H. Arenhövel, W. Leidemann and E.L. Tomusiak, Phys. Rev. C 46 (1992) 455.

[39] J.E. Amaro, J.A. Caballero, T.W. Donnelly, F. Kazemi Tabatabaei, in preparation.

[40] F. Kazemi Tabatabaei, J.E. Amaro, J.A. Caballero, Phys. Rev. **C68** (2003) 034611.

[41] J.A. Caballero, T.W. Donnelly, E. Moya de Guerra, J.M. Udías, Nucl. Phys. **A632** (1998) 323.

[42] J.A. Caballero, T.W. Donnelly, E. Moya de Guerra, J.M. Udías, Nucl. Phys. **A643** (1998) 189.

[43] M.C. Martínez, J.A. Caballero, T.W. Donnelly, Nucl. Phys. **A 707** (2002) 83; **A 707** (2002) 121.

[44] J.R. Vignote, M.C. Martínez, J.A. Caballero, E. Moya de Guerra, J.M. Udías, Phys. Rev. **C70** (2004) 044608.

[45] T. de Forest, Nucl. Phys. **A392** (1983) 232.

[46] J.E. Amaro, M.B. Barbaro, J.A. Caballero, in preparation.

[47] J.E. Amaro, J.A. Caballero, T.W. Donnelly, E. Moya de Guerra, Nucl. Phys. **A 611** (1996) 163.